Biochimica et Biophysica Acta 1807 (2011) 348–358

Contents lists available at ScienceDirect

Biochimica et Biophysica Acta

journal homepage: www.elsevier.com/locate/bbabio

Explaining the enigmatic K_M for oxygen in cytochrome *c* oxidase: A kinetic model

K. Krab [a,*], H. Kempe [a], M. Wikström [b]

[a] Department of Molecular Cell Physiology, Netherlands Institute for Systems Biology, VU University Amsterdam, Amsterdam, The Netherlands
[b] Helsinki Bioenergetics Group, Structural Biology and Biophysics Programme, Institute of Biotechnology, University of Helsinki, Helsinki, Finland

ARTICLE INFO

Article history:
Received 17 October 2010
Received in revised form 21 December 2010
Accepted 26 December 2010
Available online 3 January 2011

Keywords:
Cytochrome *c* oxidase
Kinetic model
Membrane potential
Oxygen affinity
Mitochondria
Metabolic control analysis

ABSTRACT

We present a mathematical model for the functioning of proton-pumping cytochrome *c* oxidase, consisting of cyclic conversions between 26 enzyme states. The model is based on the mechanism of oxygen reduction and linked proton translocation postulated by Wikström and Verkhovsky (2007). It enables the calculation of the steady-state turnover rates and enzyme-state populations as functions of the cytochrome *c* reduction state, oxygen concentration, membrane potential, and pH on either side of the inner mitochondrial membrane. We use the model to explain the enigmatic decrease in oxygen affinity of the enzyme that has been observed in mitochondria when the proton-motive force is increased. The importance of the 26 transitions in the mechanism of cytochrome oxidase for the functional properties of cytochrome oxidase is compared through Metabolic Control Analysis. The control of the K_M value is distributed mainly between the steps in the mechanism that involve electrogenic proton movements, with both positive and negative contributions. Positive contributions derive from the same steps that control enzyme turnover rate in the model. Limitations and possible further applications of the model are discussed.

1. Introduction

The terminal enzyme of the mitochondrial respiratory chain, cytochrome *c* oxidase (EC 1.3.3.1), catalyses the reaction:

$$4\text{cyt } c^{2+} + 8H^+_M + O_2 \rightarrow 4\text{cyt } c^{3+} + 4H^+_C + 2H_2O$$

In addition to the redox part of the reaction (oxidation of cytochrome *c* by molecular oxygen) protons are transported from the mitochondrial matrix (M) to the intermembrane space (C).

The enzyme is characterised by an apparent high affinity for its substrate oxygen. Early studies [1–3] have shown that the enzyme as studied in mitochondria has a K_M value for molecular oxygen well below 1 μM in uncoupled mitochondria. The apparent high affinity is not due to tight binding to the active site; on the contrary, the dissociation constant is high, about 0.28 mM [4]. Instead, the low Michaelis constant is due to fast trapping of the already bound O_2 [5,6]. Intriguingly, under conditions where energy back-pressure (proton motive force) is high and the redox potential difference across the respiratory chain is small, the apparent affinity for oxygen decreases, and K_M values in the 1–10 μM range are observed [2,3]. This apparent change in affinity is difficult to understand without a more or less complete description of the kinetics of cytochrome *c* oxidase. Unfortunately, kinetic models for this enzyme that incorporate all features of Gibbs energy transduction are scarce and in various system-biology models that include mitochondrial respiration the cytochrome *c* oxidase reaction has been rather sketchily represented [7–17].

Here we try to improve on this situation, not by producing a model that explains all known cytochrome *c* oxidase kinetics, but by a model that is consistent with recent advances in knowledge about the mechanism and that reproduces the K_M change upon energisation.[1]

2. The model

2.1. State description of the model

The reaction cycle is derived from the ideas expressed by Wikström and Verkhovsky [18], neglecting side paths and shortcuts [18,19]. Accordingly, the cycle is divided into 6 parts as:

1. $R_{00} + O_2 \rightarrow A_{00}$

2. $A_{00} \rightarrow P_{00}$

Abbreviations: pH_M, pH at matrix side of the membrane; pH_C, pH at cytoplasmic side of the membrane; $\Delta\psi$, membrane potential difference (C *minus* M); $\Delta\mu_{H^+}$, electrochemical potential difference for protons (C *minus* M)

* Corresponding author. Department of Molecular Cell Physiology, VU University Amsterdam, De Bolelelaan 1085, 1081 HVAmsterdam, The Netherlands. Tel.: +31 205987168; fax: +31 205987229.
E-mail address: klaas.krab@falw.vu.nl (K. Krab).

[1] The model is available as Excel file at http://www.bio.vu.nl/microb/personnel/htm/oxidase_KKM_2011.xls.

0005-2728/$ – see front matter © 2011 Elsevier B.V. All rights reserved.
doi:10.1016/j.bbabio.2010.12.015

3. $P_{00} + c^{2+} + 2H^+_M \rightarrow F_{00} + c^{3+} + H^+_C$ (+2 charges)

4. $F_{00} + c^{2+} + 2H^+_M \rightarrow O_{00} + c^{3+} + H^+_C$ (+2 charges)

5. $O_{00} + c^{2+} + 2H^+_M \rightarrow E_{00} + c^{3+} + H^+_C + H_2O$ (+2 charges)

6. $E_{00} + c^{2+} + 2H^+_M \rightarrow R_{00} + c^{3+} + H^+_C + H_2O$ (+2 charges)

The total reaction is:

$$4c^{2+} + O_2 + 8H^+_M \rightarrow 4c^{3+} + 2H_2O + 4H^+_C \quad (+8 \text{ charges})$$

The number of charges transported across the inner mitochondrial membrane is given in parentheses. In this description, the states of the enzyme are indicated by the usual letters (R, A, P, F, O and E), but added to this is a two-digit index number. Division of reaction 5, the O to E transition, into 6 steps to describe the proton pumping mechanism [18] clarifies our use of this index number:

5a. $O_{00} + c^{2+} \rightarrow O_{01} + c^{3+}$

reduction of Cu_A by cytochrome *c*; not electrogenic

5b. $O_{01} \rightarrow O_{02}$ $(+q_2$ charges)

transfer of e^- from Cu_A to heme *a*; electrogenic by fraction q_2

5c. $O_{02} + H^+_M \rightarrow O_{03}$ $(+q_3$ charges)

uptake of a vectorial proton to X (the proton-loading site) ; electrogenic by fraction q_3

5d. $O_{03} \rightarrow O_{04}$

transfer of e^- from heme *a* to heme a_3; not electrogenic

5e. $O_{04} + H^+_M \rightarrow O_{05} + H_2O$ $(+(1\text{-}q_2)$ charges)

uptake of a scalar H^+ into the binuclear center; electrogenic by fraction $1–q_2$

5f. $O_{05} \rightarrow E_{00} + H^+_C$ $(+(1-q_3)$charges)

release of vectorial H^+ from X; electrogenic by fraction $1–q_3$ 6-fold divisions of reactions 3, 4 and 6 are modelled on this, which together with data from Wikström and Verkhovsky [18] yields the state description in Table 1. We have assumed that in the P-state the electron from heme *a* is passed via heme a_3 to the tyrosine in the binuclear center (P_{03} to P_{04} to P_{05} transitions); in the F- and E-states the electron remains at heme a_3 (creating ferric and ferrous heme a_3 in F and E state, respectively).

In Fig. 1 the cycle of transitions between the 26 states is organised and characterised in a spiral reaction scheme.

2.2. Values of model parameters

Kinetic constants for the conversions R to A to P are calculated from Refs. [20–22] as summarised in Table 2.

The equilibrium constants $O_{00} \rightarrow O_{01}$ and $O_{01} \rightarrow O_{02}$ (both simple electron transfers) are calculated from the redox midpoint potentials (E_o' at pH 7) of cytochrome *c*: 0.235 V, Cu_A: 0.250 V and heme *a*: 0.270 V.

Further estimates of equilibrium constants and lifetimes τ are taken from [18]. Kinetic constants for the 6-step conversions O to E are calculated by either of two methods:

a. If the next step is faster than the step under consideration, it is assumed that the product state of the step under consideration immediately converts into the next state. In this case, the relation between the apparent first order constants $k_{forward}$, and $k_{backward}$, τ and K_{eq} is:

$$k_{forward} = \frac{1}{\tau}$$

Table 1
26 states in the oxidase model. In grey: the path of the 4 electrons into the binuclear center. *Italic*: deduced state descriptions.

state	Cu_A	heme a	X	heme a_3	Fe ligand	Cu_B	Cu ligand	tyr
R_{00}	2+	3+	-	2+	-	1+	-	OH
A_{00}	2+	3+	-	2+	O_2	1+	-	OH
P_{00}	2+	3+	-	4+	O^{2-}	2+	OH^-	$O^•$
P_{01}	1+	3+	-	4+	O^{2-}	2+	OH^-	$O^•$
P_{02}	2+	2+	-	4+	O^{2-}	2+	OH^-	$O^•$
P_{03}	2+	2+	H^+	4+	O^{2-}	2+	OH^-	$O^•$
P_{04}	*2+*	*3+*	*H^+*	3+	*O^{2-}*	*2+*	*OH^-*	*$O^•$*
P_{05}	*2+*	*3+*	*H^+*	*4+*	*O^{2-}*	*2+*	*HOH*	O^-
F_{00}	2+	3+	-	4+	O^{2-}	2+	HOH	O^-
F_{01}	1+	3+	-	4+	O^{2-}	2+	HOH	O^-
F_{02}	2+	2+	-	4+	O^{2-}	2+	HOH	O^-
F_{03}	2+	2+	H^+	4+	O^{2-}	2+	HOH	O^-
F_{04}	*2+*	*3+*	*H^+*	3+	*O^{2-}*	*2+*	*HOH*	*O^-*
F_{05}	*2+*	*3+*	*H^+*	3+	*OH^-*	*2+*	*HOH*	*O^-*
O_{00}	2+	3+	-	3+	OH^-	2+	HOH	O^-
O_{01}	1+	3+	-	3+	OH^-	2+	HOH	O^-
O_{02}	2+	2+	-	3+	OH^-	2+	HOH	O^-
O_{03}	2+	2+	H^+	3+	OH^-	2+	HOH	O^-
O_{04}	2+	3+	H^+	2+	OH^-	2+	HOH	O^-
O_{05}	2+	3+	H^+	3+	OH^-	1+	HOH	OH
E_{00}	2+	3+	-	3+	OH^-	1+	-	OH
E_{01}	1+	3+	-	3+	OH^-	1+	-	OH
E_{02}	2+	2+	-	3+	OH^-	1+	-	OH
E_{03}	2+	2+	H^+	3+	OH^-	1+	-	OH
E_{04}	*2+*	*3+*	*H^+*	*2+*	*OH^-*	*1+*	-	*OH*
E_{05}	*2+*	*3+*	*H^+*	*2+*	*HOH*	*1+*	-	*OH*

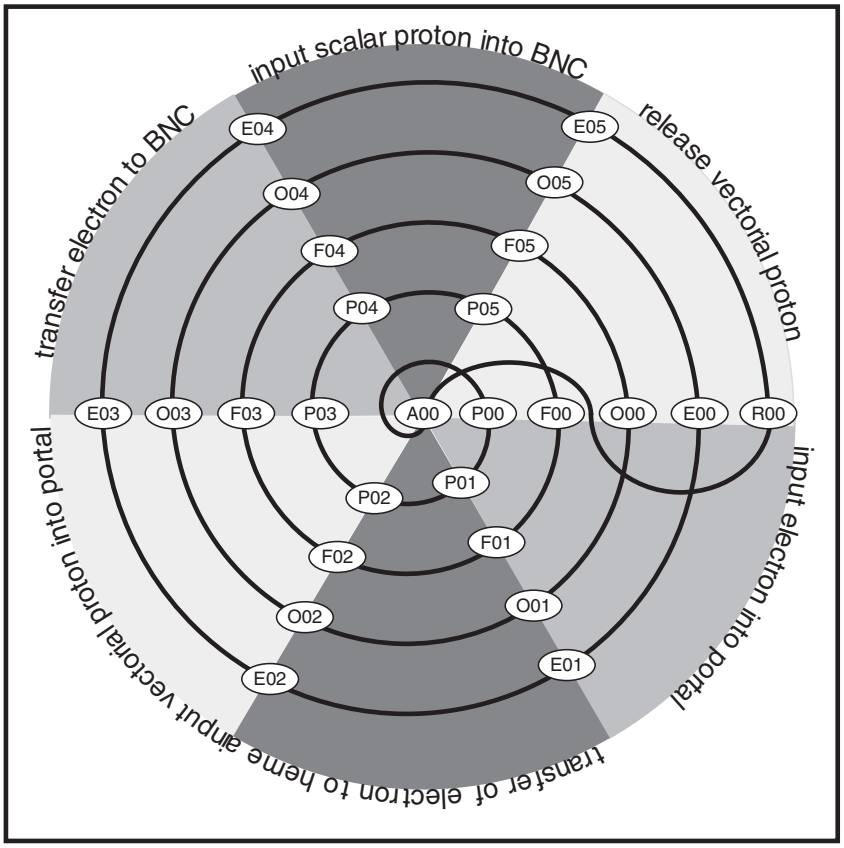

Fig. 1. Transitions in the model. BNC: binuclear center.

and

$$k_{\text{backward}} = \frac{1}{\tau \cdot K_{\text{eq}}}$$

b. If the next step is slower than the step under consideration, it is assumed that the step under consideration relaxes to equilibrium without "leakage" of the product state into the next state. In this case, the relation between k_{forward}, and k_{backward} and τ, K_{eq} is:

$$k_{\text{forward}} = \frac{K_{\text{eq}}}{\tau \cdot \left(1 + K_{\text{eq}}\right)}$$

and

$$k_{\text{backward}} = \frac{1}{\tau \cdot \left(1 + K_{\text{eq}}\right)}$$

From the apparent kinetic constants, k_{forward} ($O_{00} \rightarrow O_{01}$) was calculated with an assumed fraction $c^{2+} = 0.2$, k_{backward} ($O_{00} \rightarrow O_{01}$) was calculated with the same assumption. Note that the use of fractions of cytochrome *c* has consequences for the units in which the kinetic constants are expressed (s^{-1}). k_{forward} ($O_{02} \rightarrow O_{03}$), k_{forward} ($O_{04} \rightarrow O_{05}$) and k_{backward} ($O_{05} \rightarrow E_{00}$) all were calculated with $[H^+] = 0.1$ μM (pH = 7). The results are summarised in Table 3.

The data in Table 3 for the conversion of state O to E (reactions 5a to 5f) were extrapolated to conversions P to F, F to O and E to R. Reactions 3, 4 and 6 are considered to follow the same 6-stage pattern as reaction 5. The conversions $X_{00} \rightarrow X_{01}$, $X_{01} \rightarrow X_{02}$, $X_{02} \rightarrow X_{03}$ and $X_{05} \rightarrow Y_{00}$ do not directly involve the binuclear center (which has different configurations in the P, F, O, E states, *c.f.* Table 1) and are therefore assumed to have the same kinetics as when X is the O-state (and Y is the E-state). The remaining transitions $X_{03} \rightarrow X_{04}$ and $X_{04} \rightarrow X_{05}$ (electronic, protonic and aqueous events that directly involve the binuclear center) are summarised in Table 4.

Table 2
Thermodynamic and kinetic constants R to A to P conversions. K_{eq} calculated from ΔG, k_{forward} (R_{00} * A_{00}) calculated with $[O_2] = 100$ μM. $R = 8.314$ J mol^{-1} K^{-1}, $T = 298.15$ K. Units kinetic constants: s^{-1} except for value marked # which is in M^{-1} s^{-1}.

Transition	ΔG (kJ mol^{-1})	K_{eq}	k_{forward}	k_{backward}
$R_{00} \rightarrow A_{00}$	0 [4]	1.00×10^4 M^{-1}	1.92×10^{8} # [20]	1.92×10^4
$A_{00} \rightarrow P_{00}$	−15.07 [21]	437.25	2.80×10^4 [20]	64.04

Table 3
Thermodynamic and kinetic constants for O_{00} to E_{00} conversions. Apparent K_{eq} values at pH 7. Units kinetic constants: s^{-1} except for values marked # which are in M^{-1} s^{-1}.

Transition	K_{eq}	τ (s)	Method	k_{forward}	k_{backward}
$O_{00} \rightarrow O_{01}$	1.79	2.50×10^{-5}	a	2×10^5	1.12×10^5
$O_{01} \rightarrow O_{02}$	2.18	1.00×10^{-5}	b	6.85×10^4	3.15×10^4
$O_{02} \rightarrow O_{03}$	120	1.50×10^{-4}	a	6.67×10^{10} #	55.6
$O_{03} \rightarrow O_{04}$	1.5	1.00×10^{-9}	b	6×10^8	4×10^8
$O_{04} \rightarrow O_{05}$	16000	8.00×10^{-4}	b	1.25×10^{10} #	7.81×10^{-2}
$O_{05} \rightarrow E_{00}$	55	2.50×10^{-3}	a	400	7.27×10^{7}#

Table 4
Modification of equilibrium constants in reactions involving the binuclear center. The r factors are defined as ratios of K_{eq} in the particular state, and K_{eq} in the corresponding O-state (precise definitions can be found in the text).

Transition	$X_{03} \rightarrow X_{04}$	Factor in K_{eq}	$X_{04} \rightarrow X_{05}$	Factor in K_{eq}
$O \rightarrow E$	*heme* $a_3^{3+} \rightarrow$ *heme* a_3^{2+}	*used as standard*	$Cu_B^{2+} \rightarrow Cu_B^{1+}$ H^+ *to tyr (release of* H_2O*)*	*used as standard*
$P \rightarrow F$	heme $a_3^{4+} \rightarrow$ heme a_3^{3+}	r_{P03}	tyr $\rightarrow$ tyr$^-$ H^+ to Cu ligand	r_{P04}
$F \rightarrow O$	heme $a_3^{4+} \rightarrow$ heme a_3^{3+}	r_{F03}	no redox H^+ to Fe ligand	r_{F04}
$E \rightarrow R$	heme $a_3^{3+} \rightarrow$ heme a_3^{2+}	r_{E03}	no redox H^+ to Fe ligand (release of H_2O)	r_{E04}

The K_{eq} of the six reactions tabulated in the lower three rows of Table 4 are different from K_{eq} of the corresponding O to E transitions (first row of Table 4) by factors r_x: $K_{eq}^x = r_x \cdot K_{eq}^o$ (the index x refers to the reaction by means of its initial state, e.g. P_{04}).

For the three $X_{03} \rightarrow X_{04}$ reactions (simple electron transfers) the values of K_{eq}^x are calculated from a difference in midpoint potential between donor (heme *a*, 0.270 V) and acceptor (heme a_3, assumed values). For the two $X_{04} \rightarrow X_{05}$ reactions that are simple protonations (in F and E states), the values of K_{eq}^x are derived from assumed values of pK_a of the Fe ligand involved. The value of K_{eq} for $P_{04} \rightarrow P_{05}$ (and from it, r_{P04}) is calculated from the K_{eq} of the other 25 steps in the mechanism, and the overall K_{eq} calculated from the cytochrome *c* to O_2 redox potential difference (detailed balancing).

The above differences in K_{eq} between related reactions ultimately derive from differences in $k_{forward}$ and $k_{backward}$ between these transitions. To account for different possibilities, for each of these 6 reactions a bias factor φ_x ($-1 \le \varphi_x \le 1$) is introduced. For $\varphi_x = 1$, the difference in K_{eq} is caused by a difference in $k_{forward}$, for $\varphi_x = -1$, the difference is caused by a difference in $k_{backward}$, and for $\varphi_x = 0$ (the default value), the difference is caused by changes in both kinetic constants that are equal in size, but opposite in direction.

$$K_{eq}^x = r_x \cdot K_{eq}^o \qquad k_{forward}^x = r_x^{\left(\frac{\varphi_x + 1}{2}\right)} \cdot k_{forward}^o \qquad k_{backward}^x = r_x^{\left(\frac{\varphi_x - 1}{2}\right)} \cdot k_{backward}^o$$

Table 5 lists the parameter values and the thermodynamic and kinetic constants obtained from these operations. A complete list of these parameter values for all 26 reactions can be found in Table A1 in the Appendix.

Table 5
Arbitrary parameter values, thermodynamic and kinetic constants for conversions involving the binuclear center. Bias factors φ_x (see text) all set to 0. Units kinetic constants: s^{-1} except for values marked # which are in $M^{-1}\ s^{-1}$.

Transition	Assumption or condition	K_{eq}	$k_{forward}$	$k_{backward}$
$P_{03} \rightarrow P_{04}$	E_m(heme a_3) = 0.25 V	0.46	3.32×10^8	7.23×10^8
$P_{04} \rightarrow P_{05}$	detailed balancing	1.30×10^{11}	1.13×10^{10} #	8.66×10^{-2}
$F_{03} \rightarrow F_{04}$	E_m(heme a_3) = 0.35 V	22.5	2.32×10^9	1.03×10^8
$F_{04} \rightarrow F_{05}$	pK_a(Fe ligand) = 7	1.0×10^7	9.88×10^{7}#	9.88
$E_{03} \rightarrow E_{04}$	E_m(heme a_3) = 0.65 V	2.65×10^6	7.98×10^{11}	3.01×10^5
$E_{04} \rightarrow E_{05}$	pK_a(Fe ligand) = 6	1.0×10^6	3.12×10^{7}#	31.2

2.3. Variables in the model

Redox variables in the cytochrome *c* oxidase model are reduced cytochrome *c*, oxidised cytochrome *c*, and O_2. The former two are incorporated as fractions (cyt c^{2+} and cyt c^{3+}), essentially introducing a conserved moiety as their sum equals 1.

Variables related to energisation are free proton concentrations at the C-side and M-side, respectively, and the transmembrane electric potential difference (C-side minus M-side). The latter is incorporated as a simultaneous modifier of $k_{forward}$ and $k_{backward}$ [22], with the extra assumption that the membrane potential dependence of both kinetic constants is equal but opposite [10]. For a given fraction *q* of electrogenicity, the values of the kinetic constants then become:

$$k_{forward} = k_{forward}^o \cdot e^{\frac{-q \cdot F \cdot \Delta\psi}{2R \cdot T}}$$

and

$$k_{backward} = k_{backward}^o \cdot e^{\frac{q \cdot F \cdot \Delta\psi}{2R \cdot T}}$$

in which $k_{forward}^o$ and $k_{backward}^o$ are the rate constants at $\Delta\psi = 0$ (values in the tables).

Based on the structural information that heme *a*, heme a_3 and Cu_B are ca. one third of the membrane thickness removed from the C-side [23], electrogenicity has been distributed as follows:

- transfer of e^- from Cu_A to heme *a* (reactions $X_{01} \rightarrow X_{02}$) electrogenic by fraction $q_2 = 0.33$
- binding of vectorial H^+ from M-side to X (reactions $X_{02} \rightarrow X_{03}$) electrogenic by fraction $q_3 = 0.67$
- uptake of scalar H^+ from M-side into binuclear center (reactions $X_{04} \rightarrow X_{05}$) electrogenic by fraction $1 - q_2 = 0.67$
- release of vectorial H^+ from X to C-side (reactions $X_{05} \rightarrow Y_{00}$) electrogenic by fraction $1 - q_3 = 0.33$

2.4. Calculation of steady state

The model amounts to a cyclic scheme of 26 enzyme states (Table 1 and Fig. 1). Steady states of this model are calculated for a given set of values for the variable set {fraction cyt c^{2+}, $[O_2]$, pH_C, pH_M, $\Delta\psi$} by the method of King and Altman [24]. The procedure is implemented in an Excel document where the 676 ($= 26^2$) terms are calculated as terms of a 26×26 matrix. From these terms, the steady-state fractions of the 26 states of oxidase and the cycle flux are calculated.

2.5. Calculation of the K_M for O_2

Of the 26 conversions between the 26 enzyme states, only the forward rate of the transition $R_{00} \rightarrow A_{00}$ is dependent on (in fact, proportional to) $[O_2]$. This leads to a relation between $[O_2]$ and the steady-state rate *v* of the cycle (actually, the cycle flux) of the form:

$$v = \frac{\alpha \cdot [O_2] - \beta}{\gamma \cdot [O_2] + \delta}$$

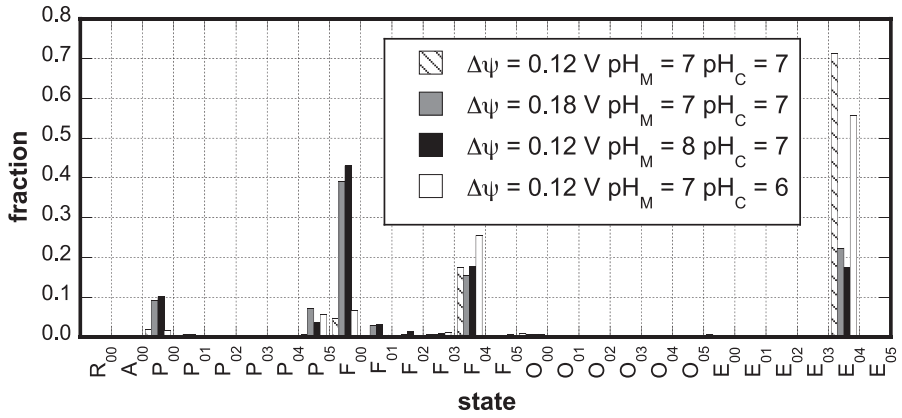

Fig. 2. States (fractions) at high and low energy state. Fraction cyt $c^{2+} = 0.04$, $[O_2] = 10^{-4}$ M, pH_C, pH_M and $\Delta\psi$ as indicated. E_m(heme a_3) = 0.25 V (in the P state), 0.35 V (in the F state) and 0.65 V (in the E state), pK_a(Fe ligand) = 7 (in the F state) and 6 (in the E state). $q_2 = 0.33$, $q_3 = 0.67$, all bias factors 0 (no bias). In the low energy state $\Delta\mu_{H^+} = 11.6$ kJ mol^{-1}, in the three high energy states $\Delta\mu_{H^+}$ = ca. 17.3 kJ mol^{-1}.

in which α is the product of the rate constants of all forward reactions, β the product of the rate constants of all reverse reactions, and γ and δ are sums of King and Altman terms (α, β, γ and δ not including $[O_2]$, but including the values of the other variables). Because $\beta << \alpha \cdot [O_2]$, this can be approximated by

$$v \approx \frac{V_{max} \cdot [O_2]}{[O_2] + K_M}$$

so that V_{max} and K_M for O_2 are calculated from the King and Altmann terms as

$$V_{max} = \frac{\alpha}{\gamma} \qquad K_M = \frac{\delta}{\gamma}$$

2.6. Control coefficients

The individual importance of the 26 transitions in the cycle for the steady-state value of system properties turnover, fractions of the cycle intermediates, K_M and V_{max} is quantified by control coefficients. These are defined for system property Z as [25]

$$C_i^Z = \frac{\partial\, lnZ}{\partial\, ln\lambda_i}$$

where λ_i is the factor by which both forward and backward rate constant of step i are changed simultaneously (c.f. [26] for a slightly different view). The advantage of this definition is that this modulation does not alter the ΔG^0 of the reaction and is hence possible through changes of catalytic/enzyme properties. Changing only

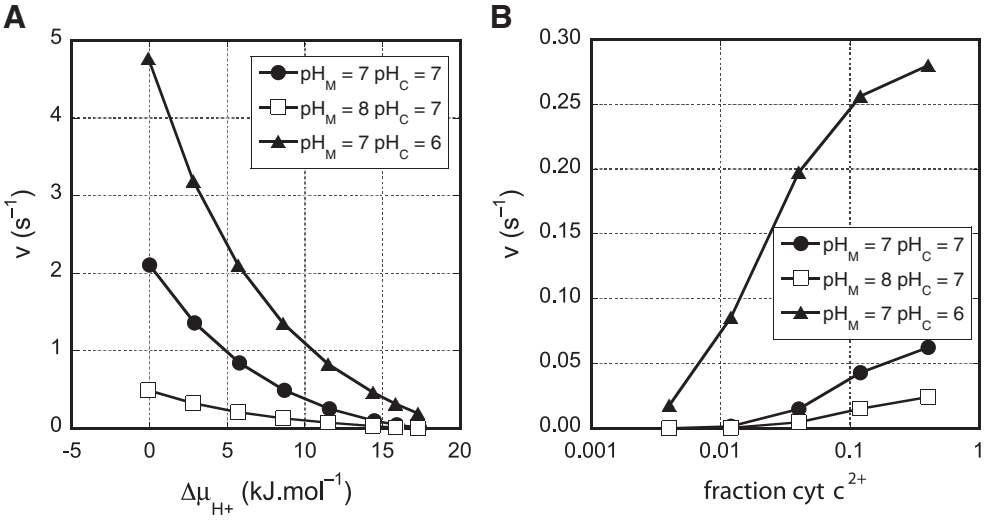

Fig. 3. Dependence of the turnover on transmembrane electrochemical potential difference for protons and cytochrome *c* reduction. A. Effect of $\Delta\mu_{H^+}$ for different fixed pH values. $\Delta\mu_{H^+}$ is varied by changing $\Delta\psi$; the fraction cyt $c^{2+} = 0.04$. B. Variation of fraction cyt c^{2+}, at $\Delta\mu_{H^+}$ = ca. 17.3 kJ mol^{-1} for different fixed pH values. $[O_2] = 10^{-4}$ M, E_m(heme a_3) = 0.25 V (in the P state), 0.35 V (in the F state) and 0.65 V (in the E state), pK_a(Fe ligand) = 7 (in the F state) and 6 (in the E state). $q_2 = 0.33$, $q_3 = 0.67$, all bias factors 0 (no bias). Note logarithmic scale for fraction cyt c^{2+} in B.

the forward or the reverse rate constant violates the second law of thermodynamics, or supposes an additional interaction with an external species. Change can be interpreted as a change in activation barrier, without effect on the ΔG of the reaction.

3. Results and discussion

3.1. Rate and enzyme states as a function of the energy state of the membrane

Fig. 2 shows the steady state distribution over the enzyme states at high and low energy state (the transmembrane electrochemical potential difference for protons, $\Delta\mu_{H^+}$) of the inner mitochondrial membrane. Cytochrome *c* is 96 % oxidised, and the difference is by an increased $\Delta\psi$ or pH_M, or by a decreased pH_C. At "low energy," only states F_{00}, F_{04} and especially E_{04} are more than 5 % populated. Raising the energy state by increasing $\Delta\psi$ from 0.12 V to 0.18 V (an increase by 5.7 kJ.mol^{-1}) additionally increases states P_{00}, P_{05}, and F_{01} to this level. This is a result which is hard to understand intuitively, as increasing $\Delta\psi$ slows down 16 out of the 26 steps in the cycle, and the resulting changes in state populations are hard to predict without a kinetic model. Increasing $\Delta\mu_{H^+}$ by raising pH_M from 7 to 8 has a similar effect on the distribution of states;

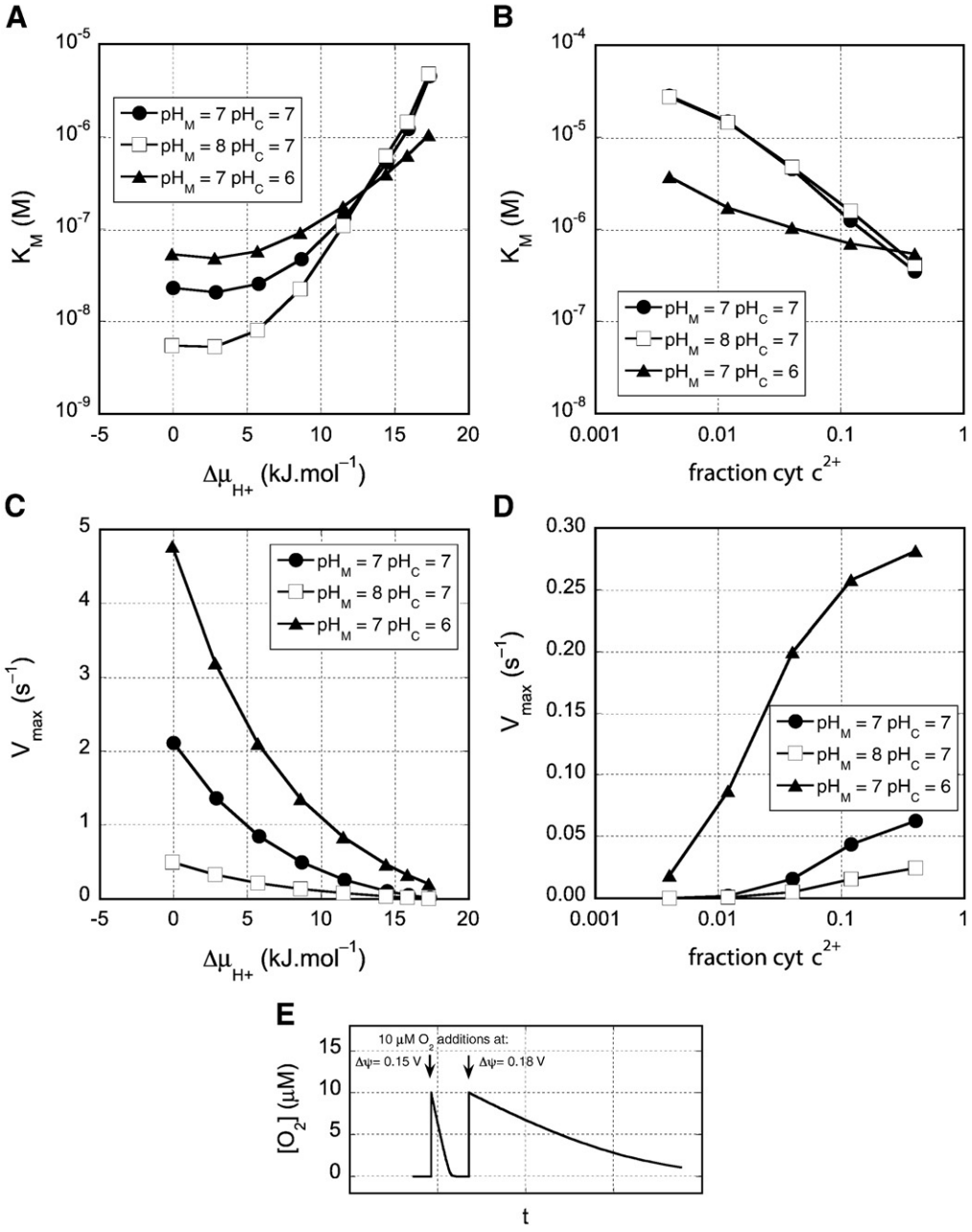

Fig. 4. Dependence of K_M for O_2 and V_{max} on energy state and cytochrome *c* reduction. A, C: Effect of $\Delta\mu_{H^+}$ for different fixed pH values. $\Delta\mu_{H^+}$ is varied by changing $\Delta\psi$; the fraction cyt $c^{2+} = 0.04$. B, D: Variation of fraction cyt c^{2+}, at $\Delta\mu_{H^+}$ = ca. 17.3 kJ mol^{-1} for different pH values. See further legend to Fig. 3. Note logarithmic scales for K_M (A, B) and fraction cyt c^{2+} (B, D). E: Simulation of oxygraph trace at high and low $\Delta\psi$. Conditions: fraction cyt $c^{2+} = 0.04$, $pH_M = pH_C = 7$, $\Delta\psi$ as indicated. E_m(heme a_3) = 0.25 V (in the P state), 0.35 V (in the F state) and 0.65 V (in the E state), pK_a(Fe ligand) = 7 (in the F state) and 6 (in the E state). $q_2 = 0.33$, $q_3 = 0.67$, all bias factors 0 (no bias). Trace calculated by integration of the kinetic expressions.

increasing $\Delta\mu_{H^+}$ by decreasing pH_C from 7 to 6 has much less effect (probably due to the additional effect of the scalar protons not being released at the C-side). A very similar pattern (increases in P_{00}, P_{01}, F_{00}, F_{01} and F_{02} at the cost of F_{04} and E_{04}, especially when $\Delta\psi$ or pH_M are increased) emerges when cytochrome *c* is in a more reduced state (not shown).

Fig. 2 suggests that (especially under low energy conditions) state E_{04} accumulates. This would lead to the prediction of a steady state in which heme a_3 is ca. 72 % reduced, which is in contrast to experimental findings. However, the overall heme a_3 redox state under these conditions is easily modified (e.g. to heme a_3^{3+}) by variation of the arbitrary parameters for heme a_3 reduction. Changing E_m(heme a_3) in the F state from 0.35 V to 0.25 V generates a low energy state (under conditions of Fig. 2) in which there is 76% heme a_3^{3+} (not shown).

The dependence of the cycle turnover rate on the different components of $\Delta\mu_{H^+}$ is shown in Fig. 3A. It is clear that the turnover rate decreases at higher energy state, but that the effects

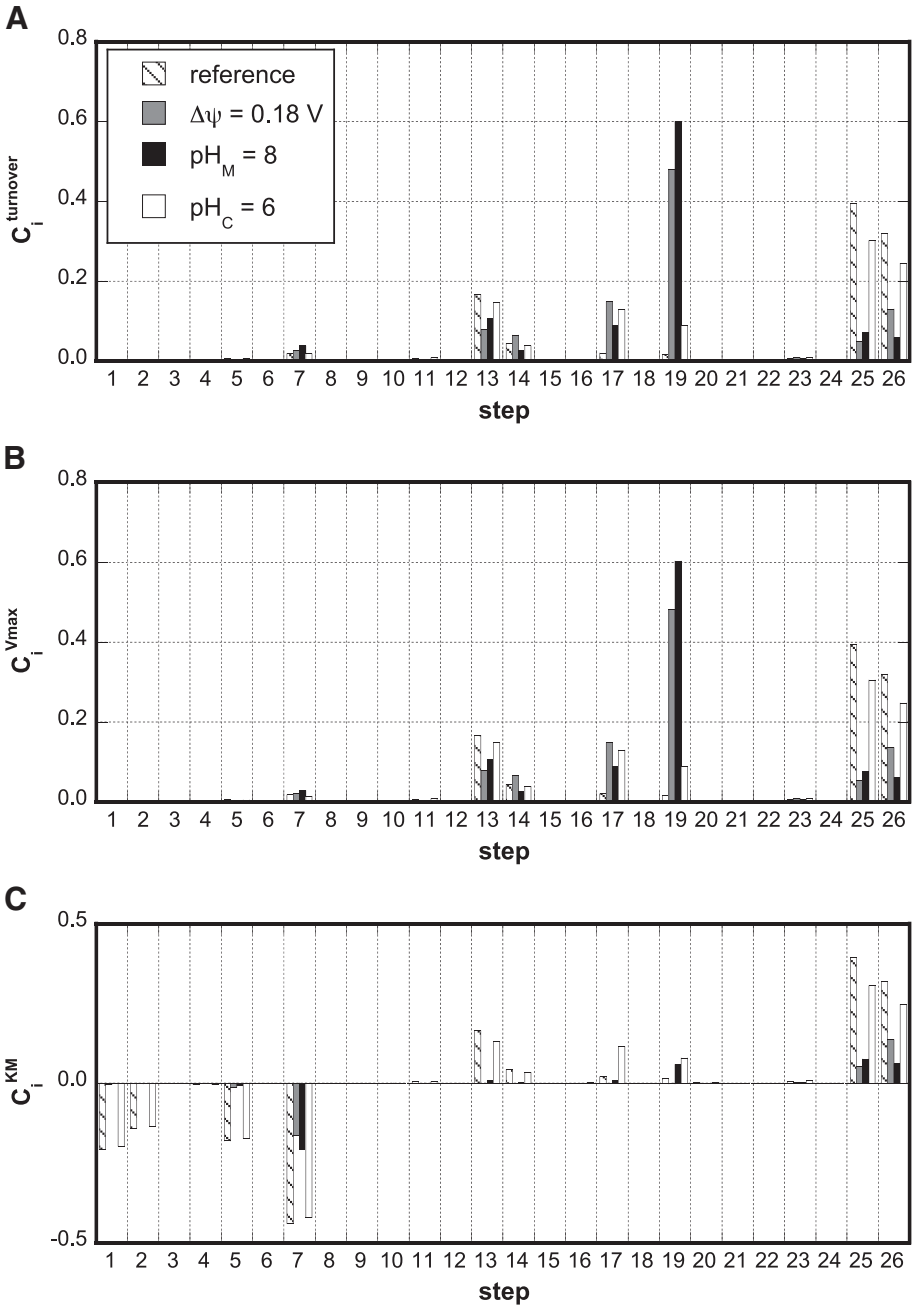

Fig. 5. Control distributions for turnover (A), V_{max} (B) and K_M (C) at high and low energy state. Steps are numbered starting from the transition of R_{00} to A_{00} (step 1). Fraction cyt c^{2+} = 0.04, $[O_2] = 10^{-4}$ M, $pH_C = 7$, $pH_M = 7$ and $\Delta\psi = 0.12$ V, unless otherwise indicated (see the panel in A). E_m(heme a_3) = 0.25 V (in the P state), 0.35 V (in the F state) and 0.65 V (in the E state), pK_a(Fe ligand) = 7 (in the F state) and 6 (in the E state). $q_2 = 0.33$, $q_3 = 0.67$, all bias factors 0 (no bias). In the low energy state $\Delta\mu_{H^+} = 11.6$ kJ mol^{-1}, in the three high energy states $\Delta\mu_{H^+}$ = ca. 17.3 kJ mol^{-1}.

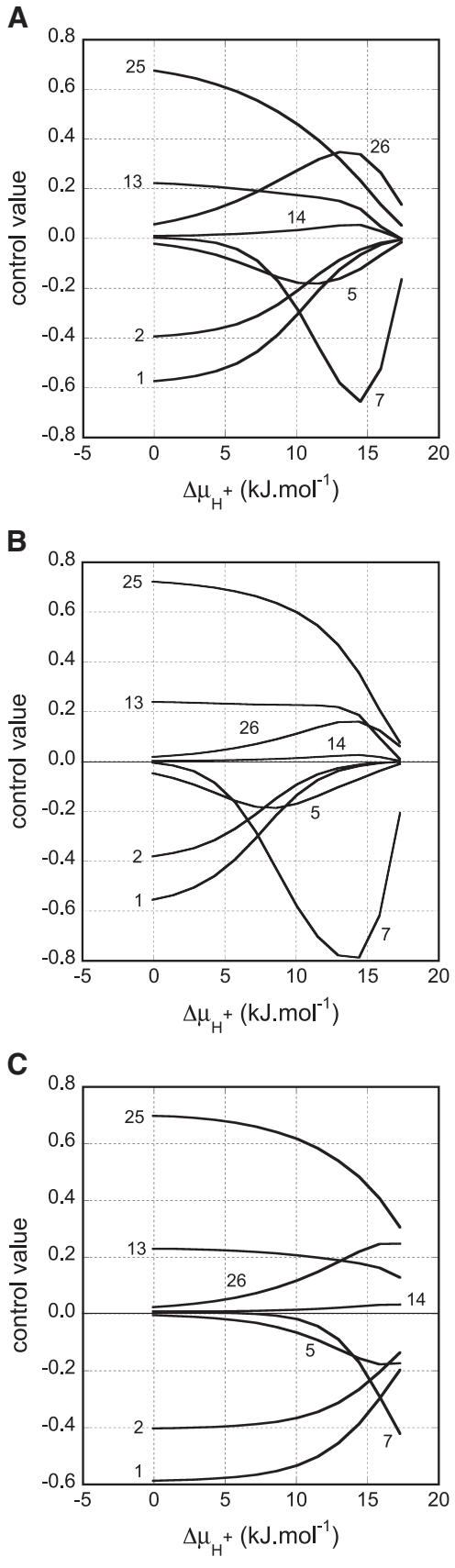

Fig. 6. Control distribution for K_M as a function of $\Delta\mu_{H^+}$. A. $pH_C = 7$, $pH_M = 7$; B. $pH_C = 7$, $pH_M = 8$; C. $pH_C = 6$, $pH_M = 7$ $\Delta\psi$ varied to generate the range of $\Delta\mu_{H^+}$. Further conditions as in Fig. 5.

of membrane potential and pH at opposite sides of the membrane are quite different and cannot be summarised in terms of an effect by $\Delta\mu_{H^+}$ as such. Fig. 3A shows that at the same value of $\Delta\mu_{H^+}$, with cytochrome *c* redox state and oxygen concentration at identical values, the rate of the cytochrome oxidase-catalysed reaction can be quite different. The data in Fig. 3A have been calculated for a very oxidised level of cytochrome *c*; Fig. 3B shows that at higher reduction levels the enzyme exhibits similar behavior.

3.2. Energy state and K_M for O_2

The model predicts a value of the K_M for oxygen that is highly sensitive to the energy state. As with the enzyme states and the turnover, effects of $\Delta\psi$, pH_M and pH_C are different.

Fig. 4A, B shows that K_M values that are less than 1 μM at lower values of $\Delta\mu_{H^+}$ increase into the micromolar range when $\Delta\mu_{H^+}$ is increased. Also, a lower reduction level of cytochrome *c* brings about an increase in K_M. These effects have also been found experimentally [3]. When the arbitrary parameters for heme a_3 reduction are varied to produce heme a_3^{3+} at low energy conditions (e.g., setting E_m (heme a_3) in the *F* state to 0.25 V) the energy-dependent K_M change persists (not shown). At lower $\Delta\mu_{H^+}$ V_{max} is higher (Fig. 4C, D). Such an effect on V_{max} is hard to determine from experimental data; if present, the experimental change in V_{max} (obtained by fitting Michaelis–Menten kinetics) seems smaller than the ones predicted by the model. Fig. 4E shows a simulation of the experimentally obtained changes in oxygen uptake kinetics in response to an increase in membrane energisation (c.f. Fig. 1 in Ref. [3]).

Because $[O_2]$ is so much in excess of the K_M-values, the pattern for turnover (Fig. 3) is the same as that for V_{max} (Fig. 4C, D).

3.3. Control of cycle flux and kinetic properties by individual steps in the mechanism

The extents to which the various steps in the reaction mechanism determine the function of cytochrome oxidase are also different in the four energy states we considered above, as quantified by the corresponding control coefficients. This is illustrated in Fig. 5 for control of cycle turnover, maximal cycle turnover (V_{max}) and K_M for oxygen. Fig. 5A clearly shows there is no individual step limiting turnover. Also, the control distribution is dependent on the energy

Table 6
Main contributions to control of turnover and K_M-value. Steps dominating control of turnover are indicated by √; steps dominating control of K_M are indicated by − (negative contribution), + (positive contribution) or var (sign dependent on energy state, but positive at low $\Delta\mu_{H^+}$).

Step	Transition	Event	$C_i^{turnover}$	$C_i^{K_M}$
1	$R_{00} \rightarrow A_{00}$	binding of O_2 to the reduced state		−
2	$A_{00} \rightarrow P_{00}$	breaking of dioxygen bond		−
5	$P_{02} \rightarrow P_{03}$	input vectorial proton		−
7	$P_{04} \rightarrow P_{05}$	input scalar proton into BNC		−
13	$F_{04} \rightarrow F_{05}$	input scalar proton into BNC	√	var
14	$F_{05} \rightarrow O_{00}$	release vectorial proton	√	var
17	$O_{02} \rightarrow O_{03}$	input vectorial proton	√	
19	$O_{04} \rightarrow O_{05}$	input scalar proton into BNC	√	var
25	$E_{04} \rightarrow E_{05}$	input scalar proton into BNC	√	+
26	$E_{05} \rightarrow R_{00}$	release vectorial proton	√	+

state: compare e.g. the effect of increasing $\Delta\psi$ or pH_M on control by step 19 vs. step 25 (both steps wherein a proton is taken up from the M-side). The same pattern is observed as with the state populations (Fig. 2): increasing $\Delta\mu_{H^+}$ by increasing $\Delta\psi$ or pH_M yields similar control distributions. However, when pH_C is decreased the distribution resembles the one at low energy state (but see Fig. 6). Control patterns for turnover and V_{max} are very similar (O_2 concentration is nearly saturating).

It is clear that the same steps (13, 14, 17, 19, 25 and 26) contribute significantly to control of all three of these entities, with the interesting exception that at the low energy state (and the high energy state with $pH_C = 6$) a number of early steps in the cycle (1, 2, 5 and 7) join in the control of K_M.

The three panels of Fig. 6 show the 8 main contributions (control values with $|C|>0.05$) to control of K_M as a function of energy state ($\Delta\mu_{H^+}$). A similar pattern is obtained irrespective of how $\Delta\mu_{H^+}$ is increased, although in Fig. 6C the pattern is shifted towards higher $\Delta\mu_{H^+}$. This shift is responsible for the apparent "low energy" behaviour of this state in Figs. 2 and 6.

In Table 6 the main contributions to control of turnover and K_M value are listed. Steps that have a large effect on turnover tend to increase the K_M for oxygen, and as such may be responsible for the lower affinity for oxygen (higher K_M) observed at high $\Delta\mu_{H^+}$.

Apart from the $R_{00} \rightarrow A_{00}$ and $A_{00} \rightarrow P_{00}$ transitions, all these steps are electrogenic proton movements. Steps that involve electron transfer from cytochrome *c* to Cu_A or heme *a* to heme a_3 (both non-electrogenic) or from Cu_A to heme *a* (electrogenic) do not contribute very much to control of either K_M or turnover. Interestingly, control of the K_M value by similar steps (e.g. input of the scalar proton into BNC) can be either negative (in the P state, step 7) or positive (in the E state, step 25). It is precisely this effect that makes it so difficult to analyse e.g. K_M changes without the help of a model such as this.

3.4. Sensitivity of K_M increase to arbitrarily chosen parameters

The main prediction of our model is the increase of K_M for oxygen upon energisation, i.e. upon an increase of the proton motive force. A number of parameters in the model (midpoint potentials of heme a_3 in the P, F, E states, pK_a of protonation of the Fe-ligand in the F, E states and 6 bias factors) have arbitrarily assigned values. Therefore, we explored how dependent the K_M change predicted by the model is on the values of these parameters, and on the charge separation parameters q_2 and q_3. We did this for each parameter by variation of its value (midpoint potentials ± 0.06 V, p*K* values ± 0.6, $q_i \pm 0.12$, bias factors ± 0.5) and calculated the K_M at high and low energy. We found that these small variations of the parameter values did not abolish the K_M difference (Fig. A1 in the appendix).

Increasing the bias factor in the protonation of the Fe-ligand in state E (step 25) decreased the V_{max} difference between the two energy states (see Fig. A1 in the appendix).

The charge separation parameters q_2 and q_3 are included in this analysis because their value is based on the assumptions that the position of group "X" involved in passing the vectorial proton is indeed close to the binuclear centre (BNC), and that the structural position of the BNC in the enzyme is reflected in its position with respect to the electrical gradient across the inner mitochondrial membrane.

3.5. Utility of the model

The unique feature of the model is that the dependence of the electron transport rate through cytochrome oxidase on membrane energisation is modelled realistically and explicitly. The model allows analysis and prediction of the separate effects of membrane potential, matrix pH and intermembrane space pH on the rate and properties of the enzyme-catalysed reaction. The model can be extended easily to include e.g. competitive inhibition of cytochrome oxidase by nitric oxide [27].

We are aware of the fact that possible subtleties of catalytic function (slip of coupling between electron transfer and proton pumping [28,29], possible function of the enzyme as a dimer, regulation of activity by the multitude of protein subunits in mammalian enzyme) are not included in the model. However, we think that the present model, which is easy to apply to different modelling environments, will be a definite improvement when the terminal reaction of respiratory electron transfer has to be incorporated in models of mitochondrial function.

It can be added that it is possible to use this model to calculate transient kinetics of the enzyme, which opens roads for further testing and improvement of the model.

Acknowledgments

The authors would like to thank H.F. Bienfait, B.W. Kooi and H.V. Westerhoff for stimulating discussions.

Appendix

Table A1
lists all thermodynamic and kinetic constant values used.

Step	Reaction	Transition	K_{eq}	$k_{forward}$	$k_{backward}$
1	1	$R_{00} \rightarrow A_{00}$	$1.00\times10^{4*}$	$1.92\times10^{8\#}$	1.92×10^{4}
2	2	$A_{00} \rightarrow P_{00}$	437.25	2.80×10^{4}	64.04
3	3a	$P_{00} \rightarrow P_{01}$	1.79	2×10^{5}	1.12×10^{5}
4	3b	$P_{01} \rightarrow P_{02}$	2.18	6.85×10^{4}	3.15×10^{4}
5	3c	$P_{02} \rightarrow P_{03}$	120 *	$6.67\times10^{10\#}$	55.6
6	3d	$P_{03} \rightarrow P_{04}$	0.46	3.32×10^{8}	7.23×10^{8}
7	3e	$P_{04} \rightarrow P_{05}$	$1.30\times10^{4*}$	$1.13\times10^{10\#}$	8.66×10^{-2}
8	3f	$P_{05} \rightarrow F_{00}$	55 **	400	$7.27\times10^{7\#}$
9	4a	$F_{00} \rightarrow F_{01}$	1.79	2×10^{5}	1.12×10^{5}
10	4b	$F_{01} \rightarrow F_{02}$	2.18	6.85×10^{4}	3.15×10^{4}
11	4c	$F_{02} \rightarrow F_{03}$	120 *	$6.67\times10^{10\#}$	55.6
12	4d	$F_{03} \rightarrow F_{04}$	22.5	2.32×10^{9}	1.03×10^{8}
13	4e	$F_{04} \rightarrow F_{05}$	1*	$9.88\times10^{7\#}$	9.88
14	4f	$F_{05} \rightarrow O_{00}$	55**	400	$7.27\times10^{7\#}$
15	5a	$O_{00} \rightarrow O_{01}$	1.79	2×10^{5}	1.12×10^{5}
16	5b	$O_{01} \rightarrow O_{02}$	2.18	6.85×10^{4}	3.15×10^{4}
17	5c	$O_{02} \rightarrow O_{03}$	120*	$6.67\times10^{10\#}$	55.6
18	5d	$O_{03} \rightarrow O_{04}$	1.5	6×10^{8}	4×10^{8}
19	5e	$O_{04} \rightarrow O_{05}$	16000 *	$1.25\times10^{10\#}$	7.81×10^{-2}
20	5f	$O_{05} \rightarrow E_{00}$	55**	400	$7.27\times10^{7\#}$
21	6a	$E_{00} \rightarrow E_{01}$	1.79	2×10^{5}	1.12×10^{5}
22	6b	$E_{01} \rightarrow E_{02}$	2.18	6.85×10^{4}	3.15×10^{4}
23	6c	$E_{02} \rightarrow E_{03}$	120*	$6.67\times10^{10\ \#}$	55.6
24	6d	$E_{03} \rightarrow E_{04}$	2.65×10^{6}	7.98×10^{11}	3.01×10^{5}
25	6e	$E_{04} \rightarrow E_{05}$	0.1*	$3.12\times10^{7\#}$	31.25
26	6f	$E_{05} \rightarrow R_{00}$	55**	400	$7.27\times10^{7\#}$

Table A1 Thermodynamic and kinetic constants for the 26 reactions of the model. Units thermodynamic constants: dimensionless, except for values marked * which are in M^{-1} and values marked ** which are in M. Values marked * or **: apparent values at pH 7. Units kinetic constants: s^{-1} except for values marked # which are in $M^{-1}\ s^{-1}$.

Figure A1, shows the influence of parameter choice and bias on the increase of K_M for O_2 upon energisation.

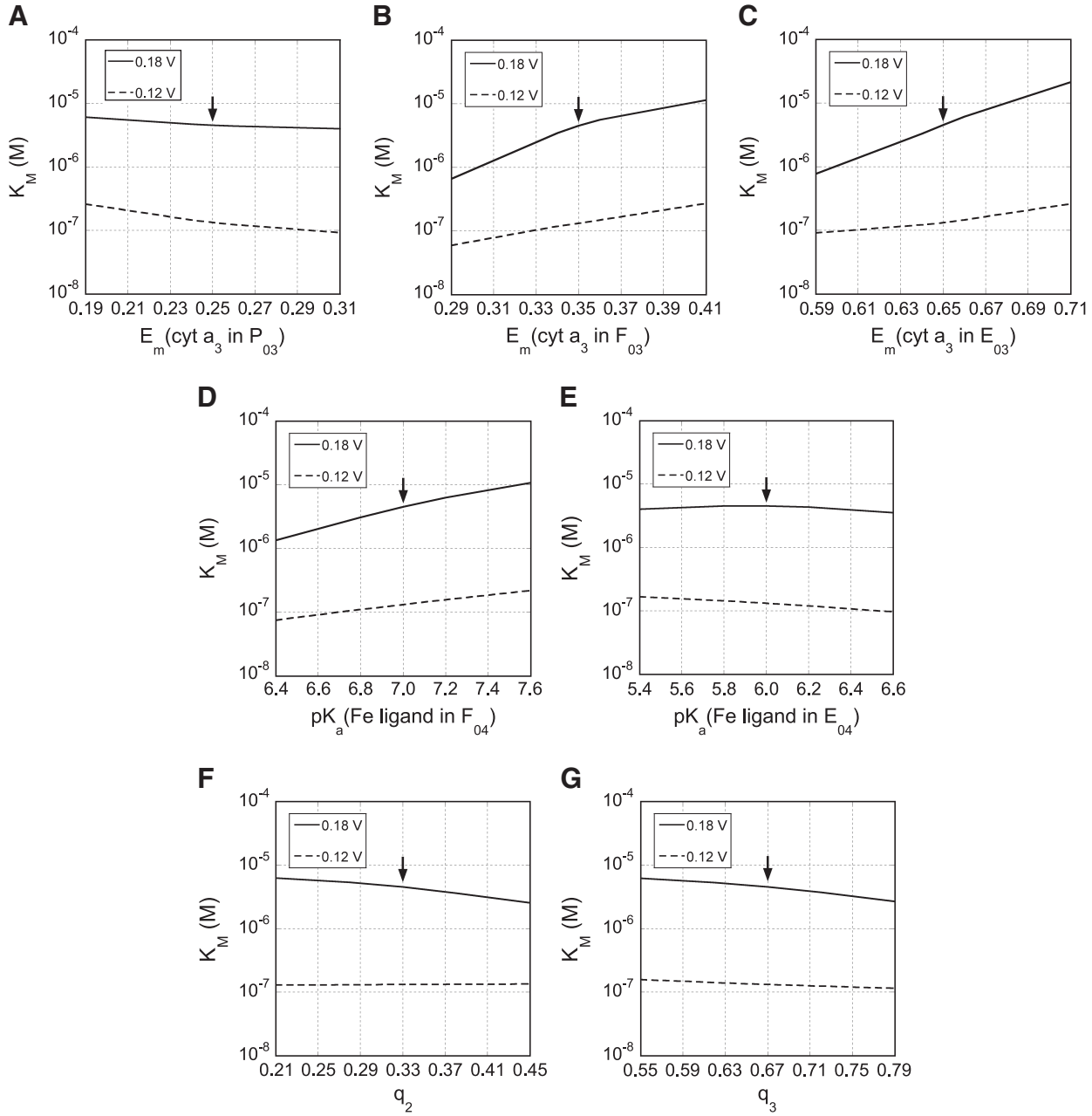

Fig. Al. The effect of parameter values and bias on oxygen kinetics. Reference situation (indicated with an arrow in the Figure panels): fraction cyt $c^{2+} = 0.04$, $[O_2] = 10^{-4}$ M, $pH_C = 7$ $pH_M = 7$ and $\Delta\psi = 0.18$ V (drawn lines) or 0.12 V (dashed lines). E_m(heme a_3) = 0.25 V (in the P state), 0.35 V (in the F state) and 0.65 V (in the E state), pK_a(Fe ligand) = 7 (in the F state) and 6 (in the E state). $q_2 = 0.33$, $q_3 = 0.67$, all bias factors $\varphi_x = 0$ (no bias). Effects on K_M of variation of arbitrary redox parameters (A–C), pK values (D, E), charge distribution factors (F, G), bias factors φ_x (H–K). Effects on V_{max} of variation of bias factors φ_x (L, M).

References

[1] H. Degn, H. Wohlrab, Measurement of steady-state values of respiration rate and oxidation levels of respiratory pigments at low oxygen tensions. A new technique, Biochim. Biophys. Acta 245 (1971) 347–355.

[2] L.C. Petersen, P. Nicholls, H. Degn, The effect of energization on the apparent Michaelis–Menten constant for oxygen in mitochondrial respiration, Biochem. J. 142 (1974) 247–252.

[3] H.F. Bienfait, J.M. Jacobs, E.C. Slater, Mitochondrial oxygen affinity as a function of redox and phosphate potentials, Biochim. Biophys. Acta 376 (1975) 446–457.

[4] M.I. Verkhovsky, J.E. Morgan, M. Wikström, Oxygen binding and activation: early steps in the reaction of oxygen with cytochrome c oxidase, Biochemistry 33 (1994) 3079–3086.

[5] B. Chance, C. Saronio, J.S. Leigh jr., Functional intermediates in the reaction of membrane-bound cytochrome oxidase with oxygen, J. Biol. Chem. 250 (1975) 9226–9237.

[6] M.I. Verkhovsky, J.E. Morgan, A. Puustinen, M. Wikström, Kinetic trapping of oxygen in cell respiration, Nature 380 (1996) 268–270.

[7] B. Korzeniewski, W. Froncisz, Theoretical studies on the control of the oxidative phosphorylation system, Biochim. Biophys. Acta 1102 (1992) 67–75.

[8] B. Korzeniewski, Simulation of oxidative phosphorylation in hepatocytes, Biophys. Chem. 58 (1996) 215–224.

[9] B. Korzeniewski, J.A. Zoladz, A model of oxidative phosphorylation in mammalian skeletal muscle, Biophys. Chem. 92 (2001) 17–34.

[10] O.V. Demin, B.N. Kholodenko, V.P. Skulachev, A model of O_2-generation in the complex III of the electron transport chain, Mol. Cell. Biochem. 184 (1998) 21–33.

[11] O.V. Demin, I.I. Goryanin, B.N. Kholodenko, H.V. Westerhoff, Kinetic modeling of energy metabolism and generation of active forms of oxygen in hepatocyte mitochondria, Mol. Biol. 35 (2001) 940–949, (Translated from Mol. Biol. (Moscow) 35 (2001) 1095-1104).

[12] S. Cortassa, M.A. Aon, R.L. Winslow, B. O'Rourke, An integrated model of cardiac mitochondrial energy metabolism and calcium dynamics, Biophys. J. 84 (2003) 2734–2755.

[13] S. Cortassa, M.A. Aon, R.L. Winslow, B. O'Rourke, A mitochondrial oscillator dependent on reactive oxygen species, Biophys. J. 87 (2004) 2060–2073.

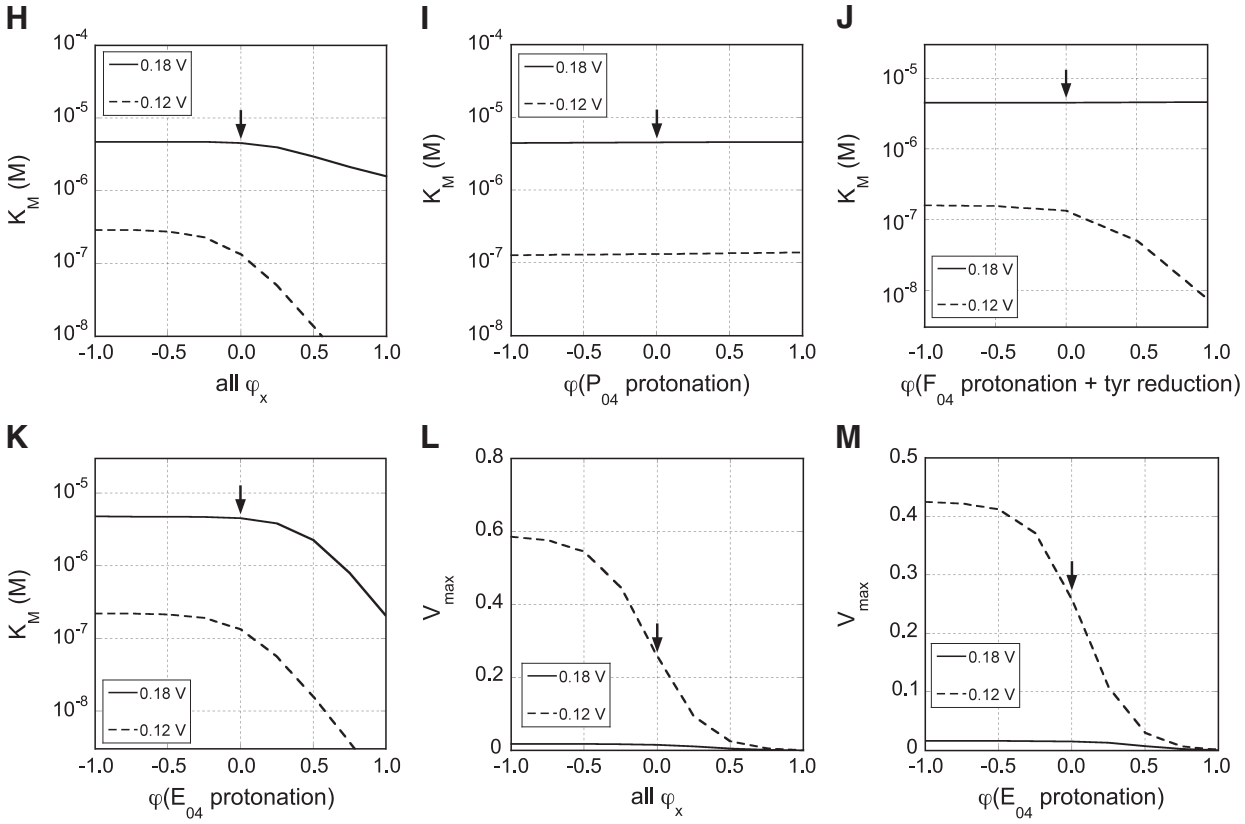

Fig. A1 (*continued*).

[14] D.A. Beard, A biophysical model of the mitochondrial respiratory system and oxidative phosphorylation, PLoS Comput. Biol. (2005) e36, Erratum in: PLoS Comput. Biol. (2006) e8.
[15] F. Wu, F. Yang, K.C. Vinnakota, D.A. Beard, Computer modeling of mitochondrial tricarboxylic acid cycle, oxidative phosphorylation, metabolite transport, and electrophysiology, J. Biol. Chem. 282 (2007) 24525–24537.
[16] D.F. Wilson, M. Stubbs, N. Oshino, M. Erecinska, Thermodynamic relationships between the mitochondrial oxidation-reduction reactions and cellular ATP levels in ascites tumor cells and perfused rat liver, Biochemistry 13 (1974) 5305–5311.
[17] P.O. Westermark, J.H. Kotaleski, A. Björklund, V. Grill, A. Lansner, A mathematical model of the mitochondrial NADH shuttles and anaplerosis in the pancreatic beta-cell, Am. J. Physiol. Endocrinol. Metab. 292 (2007) E373–E393.
[18] M. Wikström, M.I. Verkhovsky, Mechanism and energetics of proton translocation by the respiratory heme-copper oxidases, Biochim. Biophys. Acta 1767 (2007) 1200–1214.
[19] M. Wikström, M.I. Verkhovsky, Proton translocation by cytochrome c oxidase in different phases of the catalytic cycle, Biochim. Biophys. Acta 1555 (2002) 128–132.
[20] A. Sucheta, Intermediates in the reaction of fully reduced cytochrome c oxidase with dioxygen, Biochemistry 37 (1998) 17905–17914.
[21] M.R.A. Blomberg, P.E.M. Siegbahn, G.T. Babcock, M. Wikström, Modeling cytochrome c oxidase - a quantum chemical study of the O\O bond cleavage, J. Am. Chem. Soc. 122 (2000) 12848–12858.
[22] O.V. Demin, B.N. Kholodenko, V.P. Skulachev, A model of O·2- generation in the complex III of the electron transport chain, Mol. Cell. Biochem. 184 (1998) 21–33.
[23] I. Belevich, D. Bloch, N. Belevich, M. Wikström, M.I. Verkhovsky, Exploring the proton pump mechanism of cytochrome c oxidase in real time, Proc. Natl Acad. Sci. USA 104 (2007) 2685–2690.
[24] E.L. King, C. Altman, A schematic method of deriving the rate laws for enzyme-catalyzed reactions, J. Phys. Chem. 60 (1956) 1375–1378.
[25] B.N. Kholodenko, H.V. Westerhoff, Control theory of one enzyme, Biochim. Biophys. Acta 1208 (1994) 294–305.
[26] G.C. Brown, C.E. Cooper, Control analysis applied to single enzymes: can an isolated enzyme have a unique rate-limiting step? Biochem. J. (1993) 87–94.
[27] F. Antunes, A. Boveris, E. Cadenas, On the mechanism and biology of cytochrome oxidase inhibition by nitric oxide, Proc. Natl Acad. Sci. USA 101 (2004) 16774–16779.
[28] D.F. Blair, J. Gelles, S.I. Chan, Redox-linked proton translocation in cytochrome oxidase: the importance of gating electron flow. The effects of slip in a model transducer, Biophys J. 50 (1986) 713–733.
[29] S. Papa, F. Guerrieri, N. Capitanio, A possible role of slips in cytochrome C oxidase in the antioxygen defense system of the cell, Biosci. Rep. 17 (1997) 23–31.